

Characterization of the Phase Transitions of Ethyl Substituted Polyhedral Oligomeric Silsesquioxane
G. M. Poliskie¹, T. S. Haddad³, R. L. Blanski⁴, K. K. Gleason^{2}*

1. Dept of Materials Science and Eng., Massachusetts Institute of Technology Cambridge, MA 02139
2. Department of Chemical Engineering, Massachusetts Institute of Technology Cambridge, MA 02139
3. ERC Incorporated, Air Force Research Lab, Edwards Air Force Base, Edwards AFB, CA 93524
4. Air Force Research Lab, Edwards Air Force Base, Edwards AFB, CA 93524

Abstract

This study describes the synthesis and molecular mobility of both partially deuterated and fully protonated ethyl polyhedral oligomeric silsesquioxane (POSS) crystals. Phase transitions were identified with differential scanning calorimetry at ~258 K and ~253 K for partially deuterated and fully protonated ethyl POSS, respectively. A change in entropy of ~ 20.8 K was observed for both transitions. The crystallographic phase transitions were identified as a high temperature rhombohedral unit cell with a contraction in volume and symmetry described by a low temperature triclinic unit cell past the transition temperature. Abrupt changes in the spin lattice relaxation and linewidth were detected with solid state proton nuclear magnetic resonance (NMR) spectroscopy, at the same temperatures detected with calorimetry. This NMR behavior suggests a transition in molecular motions of both ethyl derivatives. For deuterated ethyl POSS, the motions become increasingly anisotropic after the temperature is lowered past its transition point. Both derivatives exhibit an increase in the correlation time ($\sim 30 \pm 2$ ns to $\sim 530 \pm 15$ ns) and activation energy ($\sim 16 \pm 2$ kJ/mol to $\sim 20 \pm 2$ kJ/mol) for molecular tumbling at temperatures past their respective transitions.

Introduction

Polyhedral oligomeric silsesquioxane (POSS) is a fused cage of cyclic siloxanes used as a nanofiller in composite research.⁷⁻¹⁰ Synthetic work has strived to functionalize the substituents on POSS molecules in order to increase its compatibility with an organic polymer matrix.¹¹⁻¹³ However, both free POSS molecules and POSS tethered to polymer chains form localized crystalline POSS domains in the polymer matrix.^{10,11} As a step toward decoupling the molecular motions of the polymer from that of the POSS, solely the molecular motions of POSS crystallites were the focus of this work.

* Corresponding Author Email: kkg@mit.edu

Report Documentation Page			Form Approved OMB No. 0704-0188		
Public reporting burden for the collection of information is estimated to average 1 hour per response, including the time for reviewing instructions, searching existing data sources, gathering and maintaining the data needed, and completing and reviewing the collection of information. Send comments regarding this burden estimate or any other aspect of this collection of information, including suggestions for reducing this burden, to Washington Headquarters Services, Directorate for Information Operations and Reports, 1215 Jefferson Davis Highway, Suite 1204, Arlington VA 22202-4302. Respondents should be aware that notwithstanding any other provision of law, no person shall be subject to a penalty for failing to comply with a collection of information if it does not display a currently valid OMB control number.					
1. REPORT DATE FEB 2005		2. REPORT TYPE		3. DATES COVERED -	
4. TITLE AND SUBTITLE Characterization of the Phase Transitions of Ethyl Substituted Polyhedral Oligomeric Silsesquioxane				5a. CONTRACT NUMBER	
				5b. GRANT NUMBER	
				5c. PROGRAM ELEMENT NUMBER	
6. AUTHOR(S) G Poleskie; T Haddad; R Blanski; K Gleason				5d. PROJECT NUMBER 2303	
				5e. TASK NUMBER 0521	
				5f. WORK UNIT NUMBER	
7. PERFORMING ORGANIZATION NAME(S) AND ADDRESS(ES) Air Force Research Laboratory (AFMC),AFRL/PRSM,10 E. Saturn Blvd.,Edwards AFB,CA,93524-7680				8. PERFORMING ORGANIZATION REPORT NUMBER	
9. SPONSORING/MONITORING AGENCY NAME(S) AND ADDRESS(ES)				10. SPONSOR/MONITOR'S ACRONYM(S)	
				11. SPONSOR/MONITOR'S REPORT NUMBER(S)	
12. DISTRIBUTION/AVAILABILITY STATEMENT Approved for public release; distribution unlimited					
13. SUPPLEMENTARY NOTES					
14. ABSTRACT This study describes the synthesis and molecular mobility of both partially deuterated and fully protonated ethyl polyhedral oligomeric silsesquioxane (POSS) crystals. Phase transitions were identified with differential scanning calorimetry at ~258 K and ~253 K for partially deuterated and fully protonated ethyl POSS, respectively. A change in entropy of ~ 20. 8 K was observed for both transitions. The crystallographic phase transitions were identified as a high temperature rhombohedral unit cell with a contraction in volume and symmetry described by a low temperature triclinic unit cell past the transition temperature. Abrupt changes in the spin lattice relaxation and linewidth were detected with solid state proton nuclear magnetic resonance (NMR) spectroscopy, at the same temperatures detected with calorimetry. This NMR behavior suggests a transition in molecular motions of both ethyl derivatives. For deuterated ethyl POSS, the motions become increasingly anisotropic after the temperature is lowered past its transition point. Both derivatives exhibit an increase in the correlation time (~30 ± 2 ns to ~530 ± 15 ns) and activation energy (~16 ± 2 kJ/mol to ~ 20 ± 2 kJ/mol) for molecular tumbling at temperatures past their respective transitions.					
15. SUBJECT TERMS					
16. SECURITY CLASSIFICATION OF:			17. LIMITATION OF ABSTRACT	18. NUMBER OF PAGES 27	19a. NAME OF RESPONSIBLE PERSON
a. REPORT unclassified	b. ABSTRACT unclassified	c. THIS PAGE unclassified			

The POSS molecule has two principle modes of rotation which includes: the rotation of the individual organic substituents edge of the cage and tumbling of the POSS cage about an axis of symmetry. In particular, rapid molecular tumbling on a three dimensional lattice is termed plastic crystalline behavior. Plastic crystals exhibit rapid molecular reorientation at high temperatures which slows to a rigid limit when cooled below a transition temperature, resulting in a small reduction in entropy (3-20 kJ/mol).^{1,2} Three-dimensional crystallographic reordering, using x-ray diffraction (XRD) and differential scanning calorimetry (DSC) can often be linked to changes in the molecular motions monitored by nuclear magnetic resonance (NMR). All three techniques have been employed to fully characterize the crystallographic, energetic and molecular motions of the plastic crystalline adamantane.³⁻⁶ Nordman and Schmitkon found adamantane went through a crystallographic phase transformation at 209 K between a high temperature cubic phase and the low temperature tetragonal phase. Furthermore, the cubic a-axis was found to have rotated 9° with respect to the c-axis of the low temperature tetragonal phase.³ Calorimetry performed by Chaung and Westrum confirmed a first order phase transition at 209 K with a change in entropy of 3.4 kJ/mol.⁴ Finally, spectroscopists, Resing⁵ and McCall, et. al.,⁶ characterized the molecular motions of these phases and found adamantane molecules underwent isotropic reorientations around the C₆ axis at room temperature. The transition to hindered molecular rotation is marked by discontinuities at 209 K in the solid state proton spin lattice relaxation time constant and spectral linewidths.^{5,6} In addition, cubane is another plastic crystal which has been fully characterized by a number of researchers using these same techniques.^{x-y} Cubane is polymorphic and characterized by two high temperature phase transitions at: 345K and 408K. Due to the similarity in the molecular architecture of cubane and POSS, it may be of interest to monitor POSS molecules as a function of temperature.

Previous work by Larsson and coworkers, has used x-ray diffraction to monitor crystallographic phase transitions in crystals of POSS containing various fully protonated organic substituents.¹⁴ Larsson notes a crystallographic phase transition of *n*-propyl POSS at 272 K from a close pack hexagonal unit cell in the high temperature phase to triclinic unit cell in the low temperature phase. Other substituents including methyl, ethyl, *i*-propyl, and *n*-butyl were also studied using the Klofer method; however, no transition was observed for these derivatives, down to the lowest experimentally accessible temperature of

243 K.¹⁴ Differential scanning calorimetry by Kopesky, et. al. identified a transition at 330 K for *i*-butyl functionalized POSS;¹⁵ however, no detailed energetic information about the phase transitions of POSS molecules has been reported. There has been no solid-state nuclear magnetic resonance spectroscopy reported on the characteristic molecular motions of these phase transitions.

In the interest of characterizing the molecular motions as a function of temperature in POSS crystallites, this paper will describe calorimetry and various solid-state NMR experiments on crystals of ethyl substituted POSS. Despite Larsson's conclusions, we have identified a phase transition in fully protonated ethyl POSS (253 K) suggesting there may be a limit to the sensitivity of the Klover method when the temperature is only dropped a few degrees below the transition point. Furthermore, ethyl substituted POSS was chosen for this study because it could be isotopically labeled from a commercially available vinyl derivative (Figure 1). A comparison between fully protonated and partially deuterated ethyl POSS illustrates how changes in chemical labeling change transition properties. In addition, deuterium NMR was used to analyze the partially deuterated derivative and provided a sensitive measure of the change in symmetry of molecular motions occurring during the phase transitions. These NMR results were confirmed with differential scanning calorimetry and x-ray crystallography.

Experimental

Synthesis of Octaethylsilsesquioxane, (CH₃CH₂)₈(Si₈O₁₂). In a glass-lined 200 mL PARR pressure reactor, 10.0 grams (15.8 mmole) of octavinylsilsesquioxane, (CH₂=CH)₈(Si₈O₁₂), was dissolved in 60 mL of dry toluene. After adding 50 mg of 10 % palladium on carbon heterogeneous catalyst, the reaction vessel was sealed, pressurized to 500 psi with 99.99% hydrogen gas, heated to 70 °C and stirred for 16 hours. The hydrogenated product was isolated by filtering the solution through celite, reducing the solvent volume and cooling the solution to -20 °C to induce crystallization. Three crops of crystals were obtained in this way, then combined together and sublimed at 150 °C under dynamic vacuum (10⁻² torr) to give 9.10 grams of product (14.0 mmole, 89 % yield). A single product is evidenced by ¹H, ¹³C and ²⁹Si NMR spectroscopy. **¹H NMR** (relative to internal CHCl₃ at 7.26 ppm): 1.00 ppm (CH₃, triplet, ³J_{H-H} = 8.0 Hz), 0.61 ppm (CH₂, quartet, ³J_{H-H} = 8.0 Hz). **¹³C NMR** (relative to internal CDCl₃ at 77.0 ppm): 6.51 ppm (CH₃), 4.08 ppm (CH₂, ²⁹Si satellites ¹J_{Si-C} = 109 Hz). **²⁹Si NMR** (relative to external SiMe₄ at 0.0 ppm): -65.5 ppm (¹³C satellites ¹J_{Si-C} = 109 Hz).

Synthesis of deuterated-Octaethylsilsesquioxane. The same hydrogenation procedure was followed except that 98% deuterium gas was used instead of hydrogen. 10 grams of octavinylsilsesquioxane was converted into 9.3 grams of partially deuterated octaethylsilsesquioxane. The product is a complex mixture of not just $(\text{CH}_2\text{DCHD})_8(\text{Si}_8\text{O}_{12})$, but contains numerous products arising from catalyst induced scrambling of the deuterium. The ^1H NMR spectrum shows an integral ratio of the methyl group to the methylene group of 1.14:1.00; the idealized product with the addition of one deuterium to each carbon would have an expected ratio of 2:1. In the ^{13}C spectrum, peaks corresponding to $\text{CH}_3\text{CH}_2\text{Si}$ groups are easily identified, and a DEPT 135 sequence ^{13}C NMR spectrum demonstrates that the methyl groups can be CH_3 , CH_2D or CHD_2 and the methylene groups can be CH_2 or CHD . Evidence for perdeuterated methyl or methylene groups was not observed. **^1H NMR** (relative to internal CHCl_3 at 7.26 ppm): 0.98 ppm (methyl, broad multiplet), 0.60 ppm (methylene, broad multiplet). **^{13}C NMR** (relative to internal CDCl_3 at 77.0 ppm): 6.52, 6.42, 6.34, 6.24, 6.15, 6.05, 5.95, 5.87, 5.77, 5.67, 5.58, 5.48, 5.39, 5.20 ppm ($\text{d}_n\text{-CH}_3$), 4.08, 3.98, 3.87, 3.80, 3.77, 3.72, 3.62, 3.52, 3.44, 3.34, 3.23 ppm ($\text{d}_n\text{-CH}_2$). **^{29}Si NMR** (relative to external SiMe_4 at 0.0 ppm): -65.4 ppm (broad multiplet).

As identified in the synthesis procedure, the 3:2 ratio for the methyl to the methylene resonances, from the solution ^1H NMR, indicated the desired fully protonated ethyl derivative was synthesized. For this reason, this product will be referred to as fully protonated ethyl POSS. Unfortunately, the deuteration of the ethyl POSS resulted in a complicated mixture of products (Figure 1). The desired deuterated ethyl product had an expected ratio of 2:1 for the methyl to methylene from solution ^1H NMR resonances. However, the ratio for the synthesized product was 1.14:1. The palladium catalyst has been known to create C-H activation^{16,17} and the deuterium gas was more than 98% pure suggesting more than on average each ethyl substituent had more than three deuterium isotopes. Despite this scrambling of isotopic products, the deuterated ethyl POSS product contained residual protons from the vinyl precursor allowing for a direct comparison of the two POSS derivatives using solid-state ^1H NMR. Therefore, the deuterated product will be referred to as partially deuterated POSS.

Single Crystal X-ray Analysis

Single crystal x-ray analysis was performed by XRD services using a single crystal of partially deuterated POSS slowly crystallized from a saturated solution of THF, the crystal had dimensions of 0.50 x

0.40 x 0.35 mm³. Measurements were made on a SMART APEX x-ray generator with Mo K α radiation and an Oxford Cryosystems 700 temperature controller. Data was analyzed using SHELX-97 software and a full matrix least squares fit on F². Goodness of fit on F² for both temperature data sets was 0.98 and 0.95 for the 290 and 110 K data, respectively. The R1 and wR2 values for all data points were 0.08 and 0.16 for the 290 K and 0.07 and 0.132 for the 110 K data sets, respectively. Full details of the crystallographic phases including bond angles, lengths and coordinates are available in other references.²⁷

Differential Scanning Calorimetry

Dynamic scanning calorimetry (DSC) was performed on a Q1000 TA instrument. Each sample was run in an aluminum pan with a step scan of two loops between 183 K and 273 K. The ramp rate was 5 K/minute. Data was analyzed using Universal Analysis software.

NMR Spectroscopy

Deuterium solid state NMR spectra were taken with a Wang 7 T magnet (with a 45 MHz ²H resonance frequency) using a Tecmag single resonance pulse generator and receiver. Static deuterium (²H) experiments were performed on a home built probe with a 2.5 μ s $\pi/2$ pulse width. Deuterium spectra were acquired with a solid echo sequence ($\pi/2$ - τ - $\pi/2$ -Acq) and a fixed delay time (τ) of 21 μ s.

Proton solid state NMR spectra were taken with an Oxford 6.3 T magnet (with a 270 MHz ¹H resonance frequency) using a Tecmag dual resonance pulse generator and receiver. Static proton (¹H) experiments were performed on a home built probe with a 2 μ s $\pi/2$ pulse width. Proton spectra were acquired with a 10 μ s dwell time and a 5 s recycle delay.

Simulations of line shapes for the static proton spectra were performed with a single peak using GRAMS® software. Simulated peaks were Gaussian with the full width half mass (FWHM) line widths extracted from the simulation.

Spin-lattice relaxations for the proton experiments were measured using an inversion recovery sequence (π - τ - $\pi/2$ -Acq). A single least square exponential was fit to the peak intensity (M) versus delay time (t), resulting in a two parameter fit yielding: the equilibrium peak intensity (M₀) and the spin-lattice relaxation time constant (T₁) (Eq 1).¹

$$Eq\ 1 : M(t)=M_0(1-2\exp(-t/T_1))$$

This single exponential was used for the POSS data with an R^2 value of ≥ 0.99 .

From the plot of $\ln T_1$ versus the inverse of temperature, the activation energies were calculated from the slope of the line (Eq 2) multiplied by the molar gas constant.¹ The slopes were taken from the most linear region of the data which created an R^2 value > 0.98 .

$$\text{Eq 2: } \ln T_1 = -E_a/(RT)$$

Results and Discussion

I. Differential Scanning Calorimetry (DSC)

The cooling and heating curves for both partially deuterated (2a) and fully protonated ethyl (2b) POSS are presented in Figure 2. For partially deuterated ethyl POSS, an endotherm and exotherm occur at 257 ± 2 K and 251 ± 2 K, respectively. For fully protonated ethyl POSS, the endotherm and exotherm occur at 254 ± 2 K and 247 ± 2 K, respectively. From the DSC scans, the change in enthalpy of the phase transition is taken from the integral of heat capacity versus temperature. Likewise, the change in entropy is estimated by dividing the enthalpy by the phase transition temperature.¹⁸ The change in enthalpy and change in of the partially deuterated POSS entropy were within error of each other for both the endotherm (5470 ± 700 Jmol⁻¹, 21.8 ± 2 Jmol⁻¹K⁻¹) and the exotherm transitions (4580 ± 700 Jmol⁻¹, 17.8 ± 5 Jmol⁻¹K⁻¹) (Table 1). The change in enthalpy (5000 ± 700 Jmol⁻¹) and change in entropy (20.2 ± 5 Jmol⁻¹K⁻¹) were identical for both phase changes of the fully protonated POSS.

Solid-solid phase transitions are commonly marked by energetic transitions identified with calorimetry.¹⁹⁻²¹ Typical values for plastic crystalline solids are a change in enthalpy of ~ 3000 - 6000 Jmol⁻¹ and a change in entropy of ~ 10 - 20 Jmol⁻¹K⁻¹, respectively.¹⁸⁻²¹ For instance previous, work by Jozkow, et. al. found a first order solid-solid phase transition for plastically crystalline pyridinium (C₅H₂NH)BiCl₄ identified by an endotherm at 119 K and an exotherm at 114 K. They found the change in entropy was 7.4 Jmol⁻¹K⁻¹, for both the observed endotherm and exotherm.¹⁹

Our results indicate that POSS undergoes a similar solid-solid phase transition with values comparable to other plastically crystalline solids. The thermal hysteresis in the heating and cooling transitions suggests the transition is first order.

II. Single Crystal X-ray Analysis

Since there is no change in the electron density between deuterated and fully protonated ethyl POSS, we have solved the crystal structure of the partially deuterated ethyl POSS to represent the expected

crystallographic phase transition for this ethyl derivative. The characteristics of the crystalline domains for each phase of the partially deuterated ethyl POSS are presented in Table 2. In the high temperature phase the unit cell can be described by a highly symmetric rhombohedral unit cell and R-3 space group while in the lower temperature phase it is best described by an asymmetric triclinic unit cell and P-1 space group. In addition to the lower symmetry of the lower temperature phase there are contractions in both the unit cell volume, from 2464.6 to $1503.58 \pm 0.05 \text{ \AA}^3$, and a decrease in the number of molecules per each unit cell, from 3 to 2 POSS molecules. This results in an 8% decrease in density from 1.3 gcm^{-3} to 1.4 gcm^{-3} .

Larsson and coworkers identified the *n*-propyl POSS phase transition at 272 K as a transition from hexagonal unit cell and R-3 space group to a triclinic unit cell and P-1 space group.¹⁴ This increase in crystallographic order was accompanied by a 10% decrease in density from 1.09 to 1.20 gcm^{-3} .¹⁴

The transition of ethyl POSS from a rhombohedral to a triclinic (Table 2) crystal structure is consistent with that observed by other researchers for *n*-propyl POSS. Furthermore, the data presented in Table 2 suggests that the crystallographic phase transition lowers the symmetry of the three dimensional molecular ordering. The contraction in the volume of the unit cell is consistent with a first order phase transition observed with calorimetry. In comparison to the *n*-propyl POSS, ethyl POSS has a higher density suggesting the smaller size of the ethyl substituent allows for a tighter packing in both phases. Nuclear magnetic resonance was undertaken in order to elucidate the dynamic molecular behavior in each of these crystallographic phases.

III. Deuterium NMR Analysis

The static ^2H NMR spectra, of the deuterated ethyl POSS at 298 K, 248 K and 243 K are shown in Figure 3. At room temperature the splitting is 6 Hz and increases to 40 Hz at 248 K. There was no change in the splitting of 40 Hz at 248 K down to our lowest experimentally accessible temperature of 203 K.

At a single orientation, the quadrupolar splitting ($\Delta\nu$) depends on to the quadrupolar coupling constant ($eQq/h \sim 200\text{kHz}$ for C-D) and the angle (θ) between the principle electronic field gradient, oriented along the C-D bond, and the magnetic field (Eq 3).¹

$$\text{Eq 3. } \Delta\nu = 3/2 (eQq/h) \langle (3\cos^2\theta - 1)/2 \rangle$$

Averaging the angle (θ) over all the C-D bonds in the molecule gives the order parameter (Eq 4).¹

$$\text{Eq 4. } P_2(\cos(\theta)) = \langle (3\cos^2\theta - 1)/2 \rangle$$

The splitting occurs when $P_2(\cos(\theta))$ is nonzero, corresponding to a situation where the electronic field gradient at the nucleus is not completely averaged to zero by molecular motions. Therefore, the order parameter is a quantitative measure of the degree of orientation in the sample.

Furthermore, the symmetry of the motions is dictated by molecular symmetry. For highly symmetric plastically crystalline compounds, such as adamantane (T_d), a combination of rotations about the C_n axis is enough to produce a symmetric isotropic 2H lineshape at room temperature.²² However, derivatives of adamantane, with a lower molecular symmetry, exhibit splitting in deuterium spectra at room temperature.²³

For our partially deuterated POSS, splitting is observed at all three temperatures with the magnitude of the splitting corresponding to a change in order parameter of the C-D bond. Figure 5 indicates an abrupt increase in the splitting from 6 Hz at 298 K to 40 Hz at 248 K. Thus, the increase in splitting (Eq 3) corresponds to greater than five-fold increase in the order parameter from 26×10^{-3} at 298 K to 133×10^{-3} at 243 K. As the temperature decreases fewer rotational states of POSS molecules are energetically accessible, leading to an increase in the order parameter (Eq 4). Therefore, the larger splitting (40 kHz) at lower temperatures indicates the molecules become more ordered and motions become increasingly anisotropic. This abrupt transition in the order parameter is consistent with a first order phase transition.

If the ethyl POSS were fully deuterated it would have a higher order of symmetry (O_h) than adamantane and therefore would be expected to have an isotropic deuterium lineshape at room temperature. However, the deuterium insertion reaction instead created a mixture of partially deuterated products of lower symmetry (Figure 1). This mixture of products, and therefore the lower molecular symmetries, most likely caused an asymmetry (6 kHz) in the lineshape due to anisotropic reorientations of the molecules at 298 K.

IV. Proton NMR Analysis

In order to analyze the motions of both types of POSS molecules, proton NMR spectra were acquired as a function of temperature. In all cases, the proton spectrum was broad and featureless; however, the width of the spectrum varied. A representative set of static proton spectra for partially deuterated and fully protonated ethyl POSS are presented in Figure 4 at three temperatures of 298, 248 and 243 K.

As seen in Figure 4, the linewidth increased with a decrease in temperature for both POSS derivatives. However, the partially deuterated POSS has a consistently smaller linewidth compared to the fully protonated POSS. A discontinuity, occurs at 258 ± 2 K for the partially deuterated ethyl POSS and 253 ± 2 K for the fully protonated ethyl POSS.

Changes in linewidth of proton spectra have previously been used to mark the phase transition of a number of plastically crystalline solids.^{1,19,24} Gutowsky and Pake found an abrupt increase in the static proton linewidth of 1,1,1-trichloroethane as it passed through a phase transition temperature at 134 K. They theorized that the proton spectrum linewidth is dependent on the frequency and type of motion of the molecule, which in turn is a function of temperature and an energy barrier for motion. Thus, they derived the following equation to relate the experimental linewidth to the underlying thermodynamic parameters (Eq 4).²⁴

$$Eq\ 4: (\delta\nu)^2 = V^2 + U^2 - V^2(2/\pi) \tan^{-1} (\alpha\delta\nu)/\nu_i$$

The linewidth ($\delta\nu$) is related to the linewidth for a rigid lattice (U), the linewidth after completion of a narrowing motion (V), a constant to correct for any inadequacies in the lineshape analysis (α), and the reorientation frequency ($\nu_i = (2\pi\tau_i)^{-1}$). Therefore, the experimental linewidth ($\delta\nu$) describes the transition between the motions of the rigid lattice (U) and motionally narrowing motions (V), limited by the thermal energy and molecular symmetry. In terms of 1,1,1-trichloroethane, Gutowsky and Pake suggested the change in linewidth would describe a transition between rigid molecules and a hindered rotation of the methyl group. In order to link the experimental linewidth to the thermodynamic parameters, Bloomberg, Pound and Purcell (BPP) theory, was used to relate the correlation time (τ_i) to the activation energy barrier for the two different modes of motion experienced in each crystallographic phase (Eq 5).^{1,24}

$$Eq\ 5: \tau_i = \tau_o \exp (-E_a/RT)$$

This assumption of Arrhenius behavior suggests that the correlation time (τ_i) is dependent on a characteristic correlation time (τ_o), activation energy (E_a), temperature (T) and the molar gas constant (R). Gutowsky and Pake's theory gives an order of magnitude approximation for the characteristics of molecular motions, specifically activation energies and correlation times. Therefore, these parameters are rarely extracted from lineshape analyses; however, this formulation provides a theoretical framework for qualitative observations. Specifically, the above equations (Eqs 4 and 5) indicate the linewidth is

proportional to the correlation time and different correlation times would describe the molecular motions on each side of the phase transition. Thus, an increase in linewidth is consistent with an increase in the correlation time for molecular tumbling as the molecules become increasingly rigid when the temperature is lowered.²⁴

Using this theory, Andrew and Eades described the increase in static proton linewidth for benzene at 100 K, as a decrease in molecular tumbling about its C_6 axis of symmetry (τ_0).²⁵ Andrew and Eades also commented on the efficiency of proton NMR to measure the differences between intramolecular and intermolecular dipolar communication of protons by comparing the linewidths of 1,3,5-partially deuterated and fully protonated benzene. The strong dipolar couplings allow for all the protons on the crystal lattice to communicate with each other prior to relaxation. Both intramolecular communication, between protons on the same substituent, and intermolecular communication, between protons on different molecules, influence the proton relaxations and linewidths. In plastic crystals, when the molecules undergo isotropic tumbling the intermolecular interactions dominate the relaxation and when the molecule becomes more rigid the intramolecular interactions dominate. Therefore, proton NMR is a behavior averaged by both intramolecular and intermolecular communication, where the observation is skewed depending on the degree of mobility in the crystal. The differences in linewidth between the two benzene derivatives gave a quantitative determination of the amount of intramolecular communication disrupted by the presence of the deuterium atoms. Qualitatively, they found that deuterated benzene had a consistently smaller linewidth than fully protonated benzene due to the decreased intramolecular dipolar interactions caused by the presence of the intermittent deuterium isotope.²⁵

Gutowsky and Pake's theory gives the correct functional dependence to describe the ethyl POSS data represented in Figure 5. Because of Eq 4 and 5, the experimental linewidth for the POSS crystals was graphed as a function of temperature. The abrupt transition observed at 258 K for deuterated ethyl POSS and 253 K for fully protonated ethyl POSS, indicate that different molecular motions, at the kilohertz frequency, dictate the linewidth prior to and after the transition. Furthermore, the increase in linewidth at low temperatures suggests molecular motions are hindered and are described by a longer correlation time past the transition point.

It should be noted that while ^1H NMR allows for a direct comparison between the two POSS derivatives, it is not the ideal choice for studying the molecular motions of phase transitions due to the extensive dipolar communication between protons. If the ethyl POSS product had been cleanly deuterated the same quantitative analysis used by Andrew and Eades²⁵ could have been performed on the POSS samples. However, our data provides the same qualitative observation that was observed for benzene. In Figure 4 and Figure 5, we observed a consistently smaller linewidth for the partially deuterated ethyl POSS. This difference between the ethyl derivatives implies the intermittent deuterium isotope decreases intracommunication between protons. Therefore, the fully protonated ethyl POSS is measurably influenced by intramolecular interactions.

These changes in molecular motions can be further characterized with the proton T_1 spin-lattice relaxation time constant, which is a sensitive measure of molecular reorientations occurring at the Larmor frequency, 270 MHz. Figures 8 and 9 are the Arrhenius plots of the $\ln T_1$ versus the inverse of temperature for the POSS molecules. For the fully protonated POSS there is a discontinuity in the graph at 253 K and for the partially deuterated POSS at 258 K. For both POSS molecules the activation energy for the low temperature region is higher than that of the high temperature region.

Using the dipolar part of the spectral density formula, the T_1 time constant is on the Larmor frequency for the ^1H isotope ($\omega = 270$ MHz) and the correlation time (τ_i) for molecular motion.¹

$$\text{Eq 6: } 1/T_1 = C \{ \tau_i / (\tau_i^2 \omega^2 + 1) + 4\tau_i / (4\tau_i^2 \omega^2 + 1) \}$$

Applying Bloomberg, Pound, and Purcell theory, inserting Eq 5 into Eq 6, suggests a plot of T_1 versus the inverse of temperature will have a minimum.^{1,24} This theory is only applicable to materials in which a single correlation time (τ_i) dictates the spin-lattice relaxation for the entire experimental temperature range. This is often not the case for solids in which a phase transition occurs in the temperature range causing different motions to dominate the relaxation in each phase.

It has been well documented for numerous solids that, when a phase transition occurs over the experimental temperature range a minimum will not be observed.^{1,5,18} Instead, as the molecular motions decrease with a decrease in temperature, there is a discontinuity in the graph at the transition temperature. For example, Resing, et. al. found that the T_1 time constants from static proton NMR of adamantane has a discontinuity in the graph at 209 K where the crystallographic phase transition occurs. At temperatures

above the transition, it is suggested that adamantane rotates freely about a C_6 axis of symmetry, described by a short correlation time and after the transition this motion is energetically less accessible, described by a longer correlation time.^{1,6}

The discontinuities, observed in Figure 6 and 7, indicate that different molecular motions of POSS dictate the relaxation of the nuclear spins prior to and after the phase transition. In addition, that transition to rigid mobility occurs at a higher temperature (258 ± 2 K) for the partially deuterated sample compared to the fully protonated sample (253 ± 2 K). Due to the scrambling of deuterated products it is difficult to conclude whether the increase in the transition temperature is the result of the heavier isotope or the identified asymmetry of the molecular structures. It is plausible that the increased mass of the deuterium labels increases the moment of inertia for the molecules decreasing the molecular tumbling in the high temperature phase. This decreased mobility would require less thermal energy to be removed in order for the molecules to become completely rigid. It is equally likely that due to the scrambling of the deuterated products, on average, the asymmetry in the POSS molecules excludes certain modes of motion; therefore, decreasing the mobility in the high temperature phase and increasing the temperature at which the molecule becomes completely rigid.

The characteristic correlation time and the activation energy for the molecular motions can be determined assuming BPP theory. When the temperature was decreased from 298 to 243 K, the characteristic correlation time (τ_o) increased from 28 ± 2 ns to 530 ± 15 ns and from 32 ± 2 ns to 520 ± 15 ns, for the partially deuterated and fully protonated POSS, respectively (Table 2). For both the fully protonated and partially deuterated ethyl POSS, the activation energy for molecular tumbling is lower at temperatures above the transition ($E_a \sim 16 \pm 2$ kJ/mol) than below ($E_a \sim 20 \pm 2$ kJ/mol) (Table 2).

Simulations of the molecular motions of POSS performed by Capaldi, et. al. determined the correlation time for isotropic molecular tumbling of a single cyclopentyl POSS molecule in a vacuum. The time scale with this random, isotropic tumbling of the POSS molecule around its C_n axis of symmetry was 5 ns. The isotropic rotation of the cyclopentyl groups had a correlation time of 120 ps.²² In addition, the activation energy, found for adamantane, where NMR has been shown to be sensitive to changes in the ability of the molecule to tumble around their C_6 axis, was ~ 22 kJ/mol.¹

Therefore, the activation energy and correlation times extracted from the spin-lattice relaxation data for our ethyl POSS, as presented in Table 3, are consistent with a more restricted tumbling of the POSS molecule around its C_n axis of symmetry. However the difference in the transition temperature suggests a difference in the degree of molecular mobility in the high temperature phase of each derivative. Therefore, the similarity in the correlation times and activation energies between the two derivatives is unexpected. It is possible that for both POSS derivatives the dipolar coupling allows the intermolecular interactions of the protons to dominate the relaxations on both sides of the transition temperature. This intermolecular communication between POSS molecules on the lattice may mask the differences in the intramolecular interactions caused by molecular tumbling. In fact, the dipolar communication could cause an average behavior of the intermolecular and intramolecular interactions to be observed. Therefore, despite the fact that the values of the activation energy and correlation times mimic C_n rotations caution needs to be taken when interpreting these experiments.

Despite the ambiguity in the interpretation of the absolute value of the correlation time and activation energy, it can be stated that both POSS molecules undergo a phase transition marked by abrupt changes in molecular motions. Furthermore, this overall increase in activation energy and correlation times with decreased temperature is consistent with restricted molecular mobility in the low temperature phase due to a lower thermal energy.

Conclusions

Phase transitions occur in ethyl POSS molecules and have been identified using calorimetry, x-ray crystallography and various NMR experiments. The transition points observed with calorimetry are identical to those observed with NMR. The high temperature phase was identified as rhombohedral and the low temperature phase was triclinic. The behavior observed with calorimetry, x-ray crystallography and NMR are typical to those of plastic crystals. The temperature of the phase transition was tuned by isotopically labeling the substituents on the POSS molecule. At higher temperatures, the molecular reorientations are rapid and for deuterated POSS slightly anisotropic. After the transition, and at lower temperatures, the molecular reorientations are slower and for deuterated POSS increasingly anisotropic.

Acknowledgement

The authors acknowledge funding from the US Air Force under Grant No. F49620-01-1-0447. We also thank XRD services for providing the crystallographic data.

References

1. Fyfe, C.A. Solid State NMR for Chemists CFC Press: Ontario 1983.
2. Sherwood, J.N. The Plastically Crystalline State New York: John Wiley and Sons 1979.
3. Nordman, C.E.; Schmitkons, D.L. Acta Cryst 1965, 18, 764.
4. Chang, S.; Westrum, E.F. J. Phys. Chem. 1960, 64, 1541.
5. Resing, H.A. Mol. Cryst. Liq. Cryst. 1969, 9, 101.
6. McCall, D.W.; Douglas, D.C. J. Chem. Phys. 1960, 33, 777.
7. Iyer, S.; Somlal, A.P.; Schiraldi, D.A. Polymeric Material Science and Engineering 2004, 90, 486.
8. Yei, D.; Kuo, S.W.; Su, Y.; Chang, F. Polymer 2004, 45, 2633.
9. Lee, A.; Lichtenhan, J.D. Macromolecules 1998, 31, 4970.
10. Jeon, H.G.; Mather, P.T.; Haddad, T.S. Polymer International 200, 49, 453.
11. Kum, K.; Chajo, Y. J Mater Chem 2003, 13, 1384.
12. Mantz, R.A.; Jones, P.F.; Chaffee, K.P.; Lichtenhan, J.D.; Gilman, J.W.; Ismail, I.M.K.; Burmeister, M.J. Chem Mater 1996, 8, 1250.
13. Murtee, H.J.; Thoms, T.P.S.; Greaves, J.; Hong, B. Inorg Chem 2001, 39, 5209.
14. Larsson, K. Arkiv Kemi 1960, 16, 209.
15. Kopesky, E.; McKinley, G.; Cohen, R.E. Macromolecules 2004 in press.
16. Pass, G.; Littlewood, A.B.; Burwell, R.L. J. Chem Phys 1960, 12, 6281.
17. Lee, T.R.; Whitesides, G.M. Acc Chem Res 1992, 25, 266.
18. Horiuchi, K.; Ishihara, H.; Hatano, N.; Okamoto, S.; Gushiken, T. Z. Naturforsch 2002, 57, 425.
19. Jozkow, J.; Medycki, W.; Zaleski, J.; Ryszard, J.; Bator, G.; Ciunik, Z. Phys. Chem. Chem. Phys., 2001, 3, 3222.
20. Wilding, M.C.; McMillan, P.F.; Navrotsky, A. Physica A 2002, 314, 379.
21. Willart, J.F.; Descamps, M.; Bertault, M.; Benzakour, N. J Phys Condens Matter 1992, 4, 9509.
22. Seeber, A.J.; Forstyh, M.; Forsyth, C.M.; Forsyth, S.A.; Annat, G.; MacFarlane, D.R. Phys. Chem. Chem. Phys., 2003, 5, 2692.
23. ManIntosh, M.R.; Fraser, B.; Gruwel, M.L.H.; Wasylishen, R.E.; Cameron, T.S. J. Phys. Chem. 1992, 96, 8572.
24. Gutowsky, H.S.; Pake, G.E., J. Chem. Phys., 1950, 18, 162.

25. Andrew, E.R.; Eades, R.G. Proc. Roy. Soc. A 1953, 216, 398.
26. Capaldi, F. PhD Thesis, Department of Mechanical Engineering, MIT 2005.
27. Dadchov, M.

List of Figures and Tables:

Figure 1. Molecular structure of ethyl POSS

Figure 2. Differential scanning calorimetry measurements of partially deuterated and fully Protonated ethyl POSS

Figure 4. Solid-state deuterium NMR spectra for partially deuterated ethyl substituted POSS as a function of temperature

Figure 5. Solid-state static ^1H spectra of fully protonated and partially deuterated ethyl POSS as a function of temperature

Figure 6. Solid-state ^1H linewidth as a function of temperature for fully protonated and partially deuterated ethyl substituted POSS

Figure 7. Solid-state ^1H spin-lattice relaxation time constants (T_1) as a function of temperature for fully protonated ethyl substituted POSS

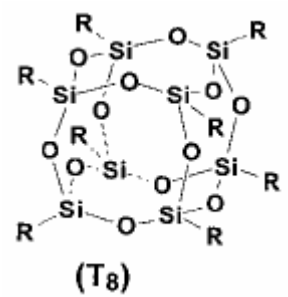
Figure 8. Solid-state ^1H spin-lattice relaxation time constants (T_1) as a function of temperature for partially deuterated ethyl substituted POSS

Table 1: Characterisitics of the phase tranistion and phase behavior of ethyl substiuted POSS extracted from DSC

Table 2. Crystallographic characteristics of each phase of the partially deuterated ethyl POSS

Table 3: Characterisitics of the phase tranistion and phase behavior of ethyl substiuted POSS from NMR

Figure 1. Molecular structure of ethyl POSS



A. Partially Deuterated Ethyl POSS



B. Fully Protonated Ethyl POSS

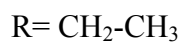


Figure 2. Differebntial scanning calorimetry measurements of partially deuterated and fully protonated ethyl POSS

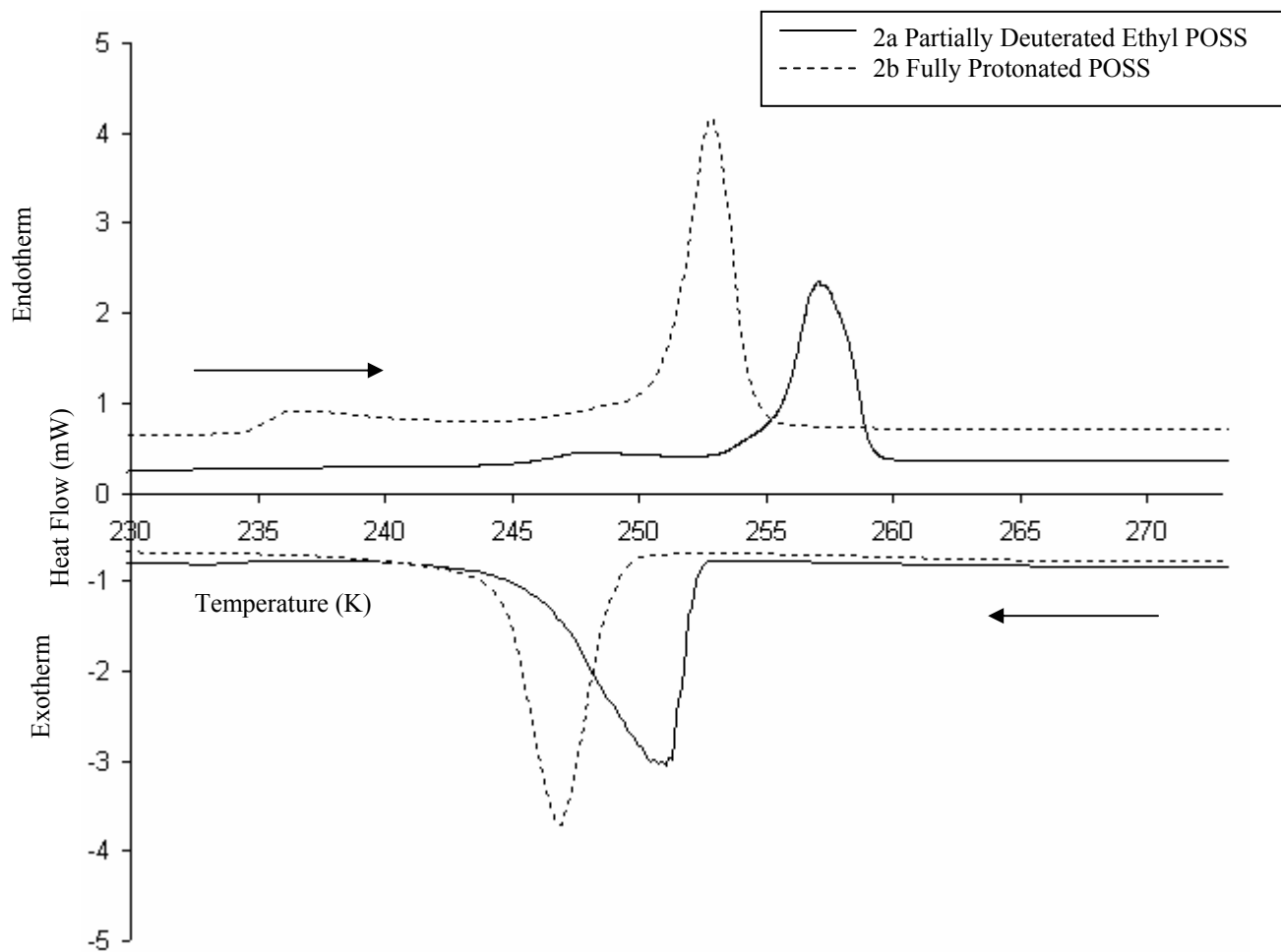


Table 1: Characteristics of the phase transition and phase behavior of ethyl substituted POSS extracted from DSC

<i>Substituent</i> *	Transition Temperature (K) (± 2 K)	ΔH (Jmol⁻¹) (± 500 Jmol⁻¹)	ΔS (Jmol⁻¹K⁻¹) (± 2 Jmol⁻¹ K⁻¹)
CHDCH ₂ D	Texo = 257	4580	17.8
	Tendo = 251	5470	21.8
CH ₂ CH ₃	Texo = 254	5000	20.2
	Tendo = 247	5000	20.2

* H stands for ¹H and D stands for ²H isotope

Table 2. Crystallographic characteristics of each phase of the partially deuterated ethyl POSS

Cell Characteristics	Phase I 290 ± 2 K	Phase II 110 ± 2 K
Crystal System	Rhombohedral	Triclinic
a (Å)	13.998 ± 0.002	9.7005 ± 0.0007
b (Å)	13.998 ± 0.002	12.1558 ± 0.0009
c (Å)	14.53 ± 0.02	13.0907 ± 0.0010
α (°)	90	87.850 ± 0.002
β (°)	90	88.024 ± 0.002
γ (°)	120	77.187 ± 0.002
Z (molecules/cell)	3	2
Volume (Å ³)	2464.6	1503.58
Density (gcm ⁻³)	1.3	1.4
Possible Space Groups	R-3	P-1

Figure 3. Solid-state deuterium NMR spectra for partially deuterated ethyl substituted POSS as a function of temperature

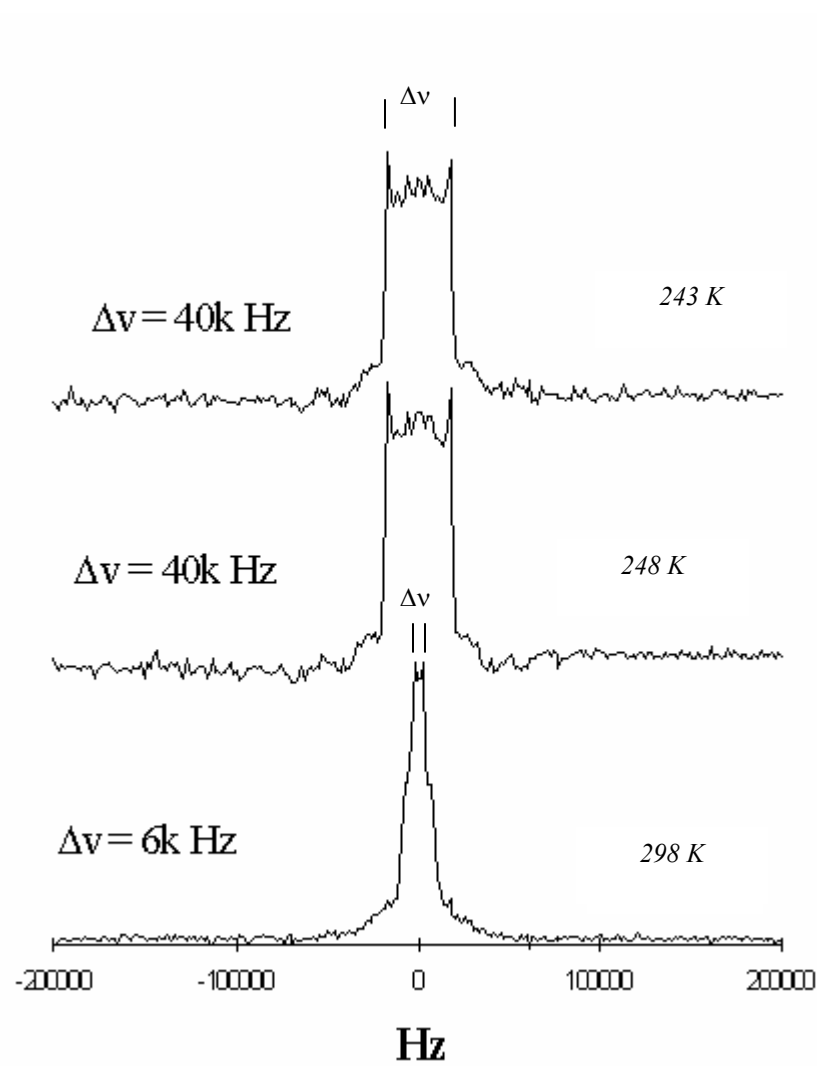


Figure 4. Solid-state static ^1H spectra of fully protonated and partially deuterated ethyl POSS as a function of temperature

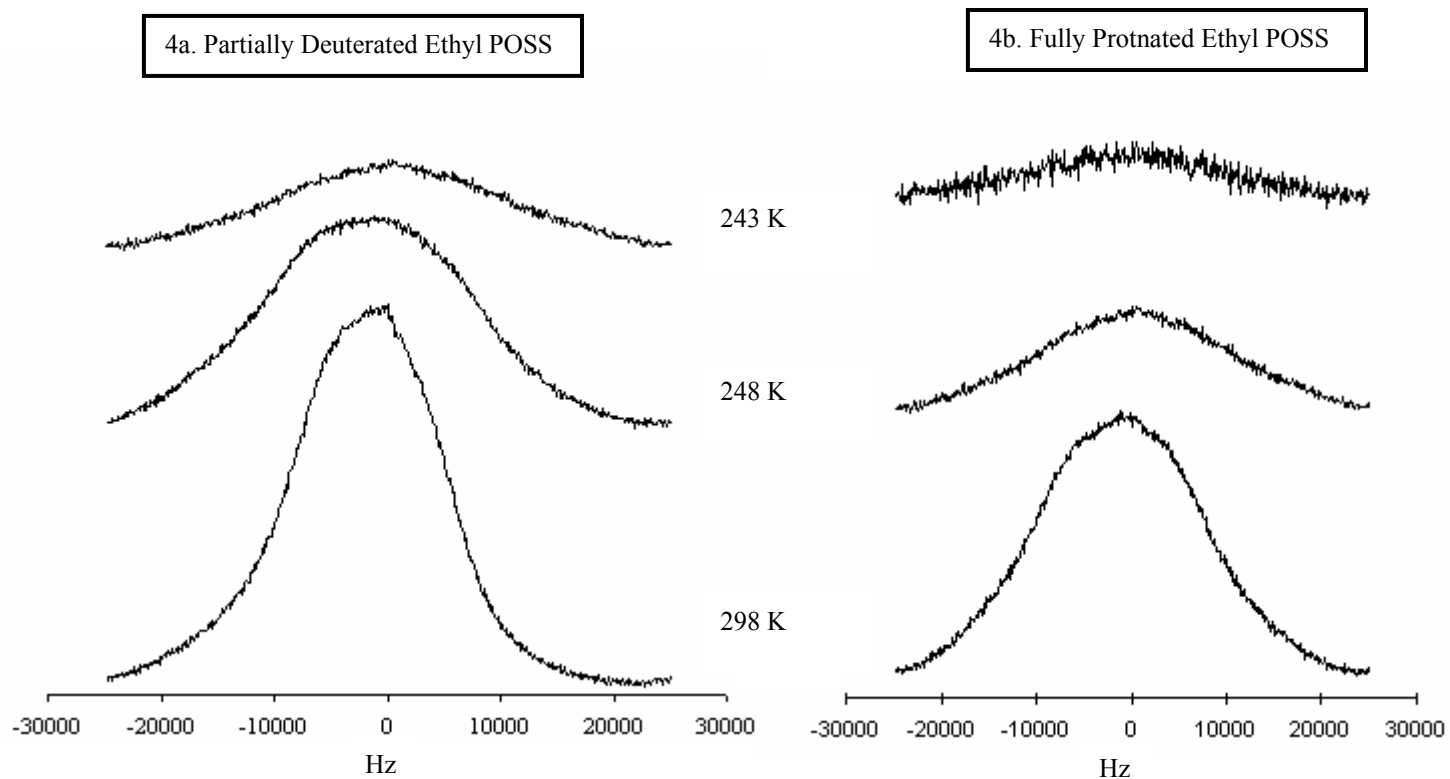


Figure 5. Solid-state ^1H linewidth as a function of temperature for fully protonated and partially deuterated ethyl substituted POSS

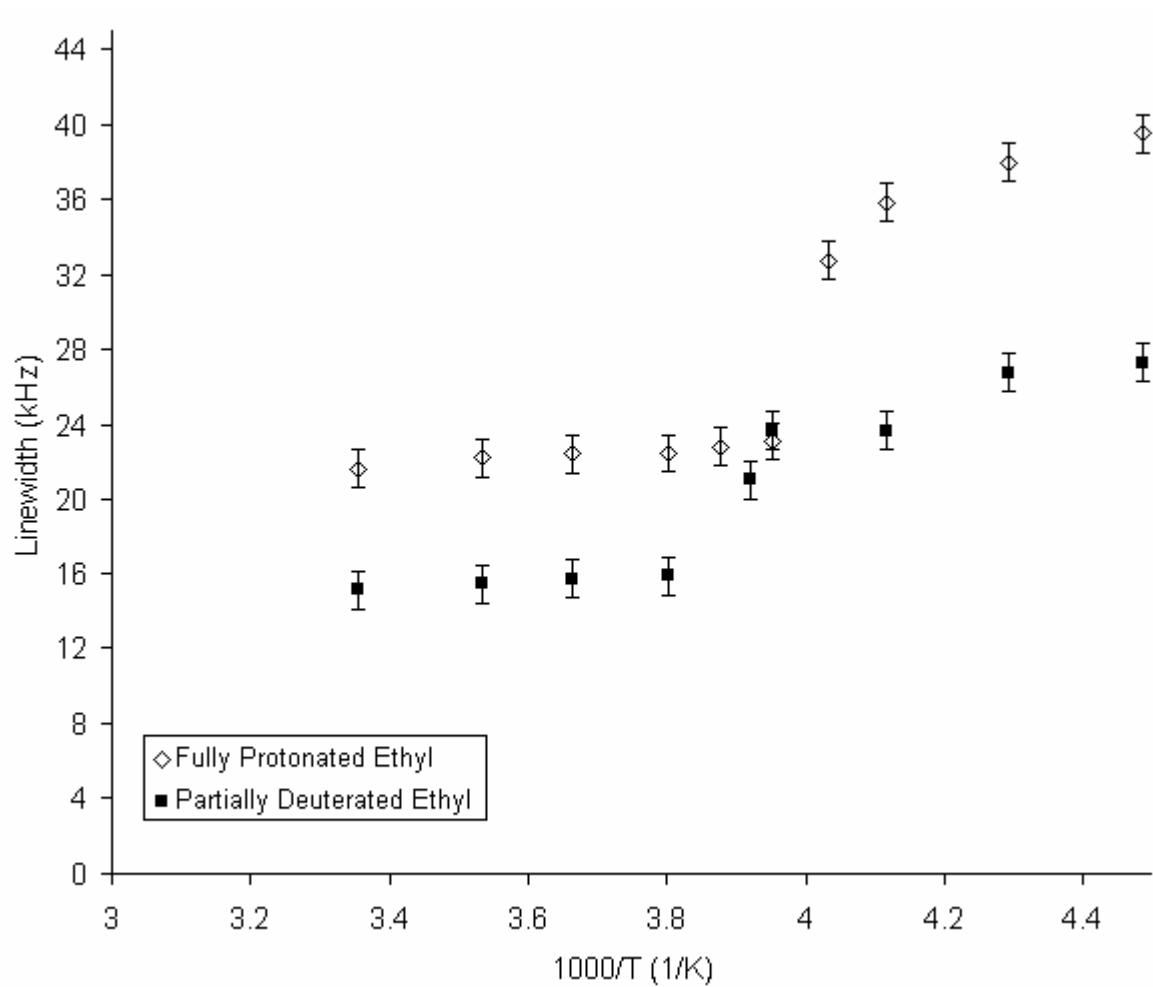


Figure 6. Solid-state ^1H spin-lattice relaxation time constants (T_1) as a function of temperature for fully protonated ethyl substituted POSS

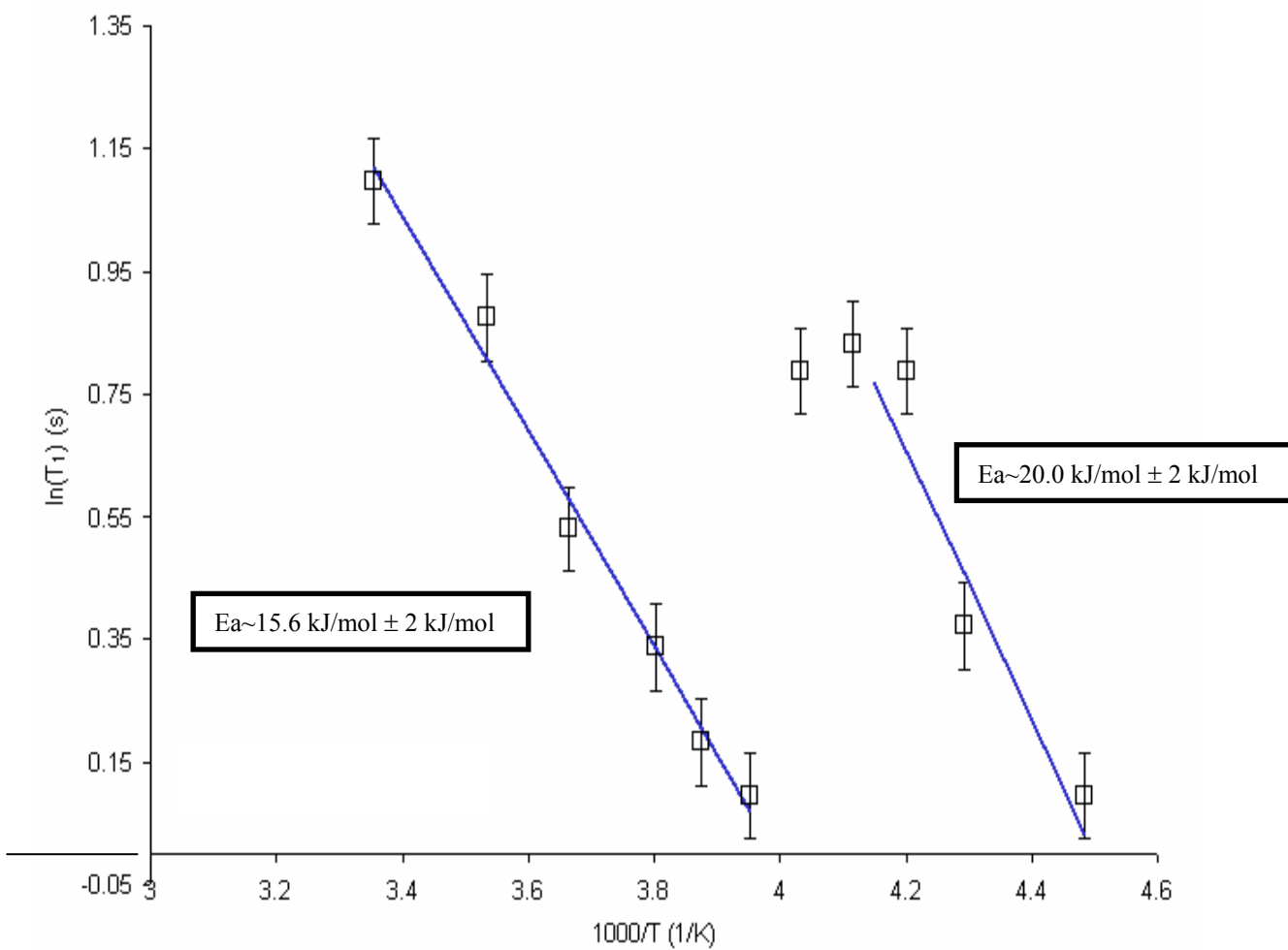


Figure 7. Solid-state ^1H spin-lattice relaxation time constants (T_1) as a function of temperature for partially deuterated ethyl substituted POSS

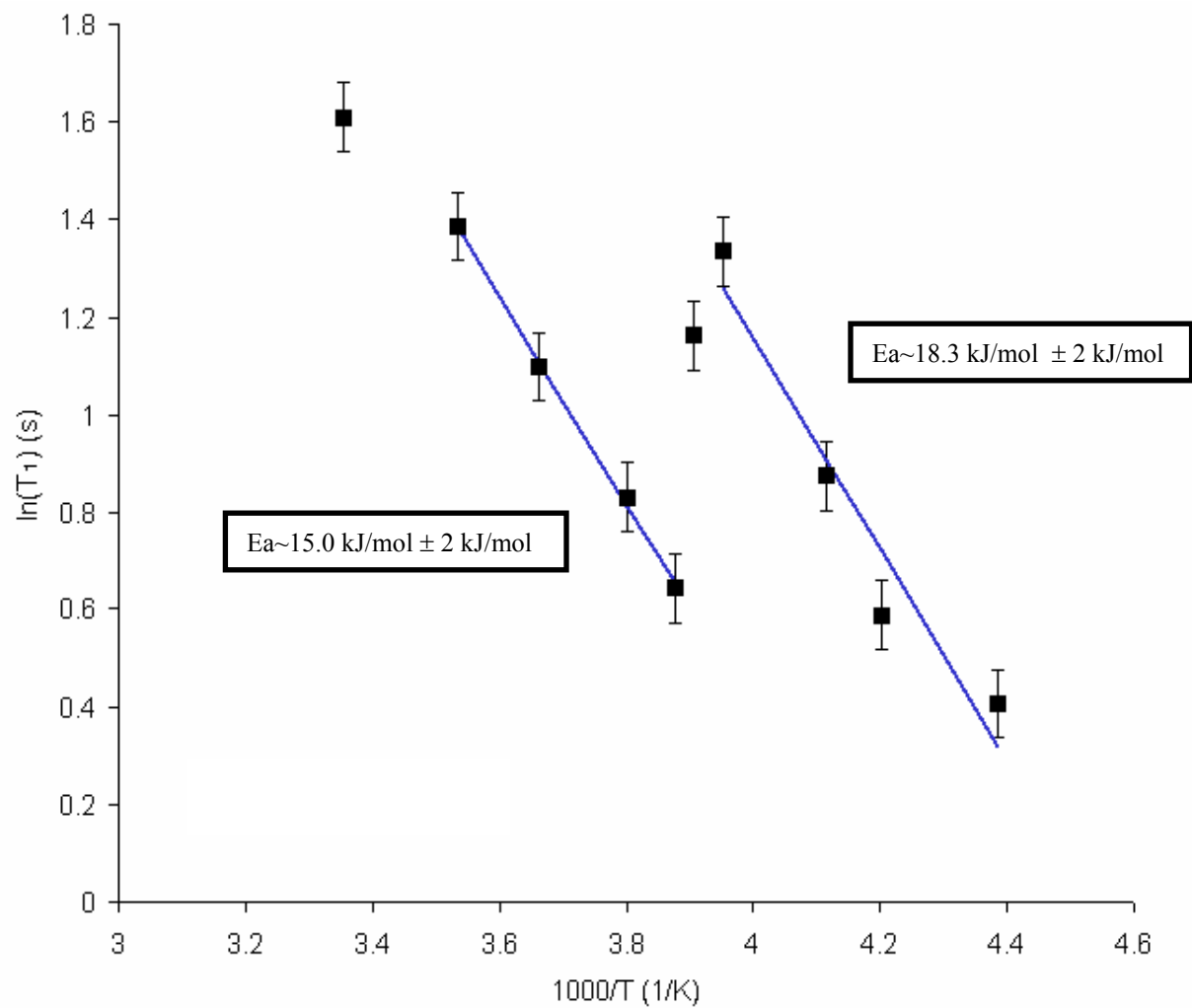


Table 3: Characterisits of the phase tranistion and phase behavior of ethyl substiuted POSS from NMR

<i>Substituent</i> *	Transition Temperature in NMR (K) (± 2 K)	Ea (kJ/mol) Phase I (high temperature) (± 2.0 kJ/mol)	Ea (kJ/mol) Phase II (low temperature) (± 2.0 kJ/mol)	τ_0 Phase I (25 °C) (ns) (T_1) (± 2 ns)	τ_0 Phase II (-30 °C) (ns) (T_1) (± 15 ns)
CHDCH ₂ D	258	15.0	18.3	28 ($T_1 \sim 5$ s)	530 ($T_1 \sim 2$ s)
CH ₂ CH ₃	253	15.6	20.0	32 ($T_1 \sim 3$ s)	520 ($T_1 \sim 2$ s)

* H stands for ¹H and D stands for ²H isotope